

Supporting Information: Electrochemical reduction of CO₂ on Ir_xRu_(1-x)O₂ (110) surfaces

Arghya Bhowmik, Dr. Heine Anton Hansen* and Prof. Dr. Tejs Vegge

Department of Energy Conversion and Storage, Technical University of Denmark, Fysikvej Bldg. 309,

DK-2800 Kgs. Lyngby, Denmark.

E-mail: heih@dtu.dk; Fax: +45 46 77 57 58; Tel: +45 45 25 82 11

Computational details

Simulation parameters

The density functional theory (DFT) based simulation tool Vienna ab-initio simulation package (VASP)¹, is used here. 500 eV cutoff is used for wave functions. The bulk IrO₂ or RuO₂ unit cell Brillouin zone is sampled with a 5×5×7 Monkhorst-Pack k-point mesh and that of the oxide catalyst surface slab is 4×4×1. The catalyst surface model consists of four atomic (metal and oxygen atoms) layer thick slab, which is periodic in x and y direction. The simulation cell dimensions are 6.399 Å × 6.451 Å × 27.902 Å for models with IrO₂ substrate and 6.271 Å × 6.416 Å × 27.831 Å for models with RuO₂ substrate. Due to periodic boundary conditions, 16 Å of vacuum in the z-direction is considered to minimize spurious interlayer interactions. Due to the finite electronic occupation at Fermi energy, a Gaussian smearing of 10 meV is used for the electronic states in all calculations. Optimizations of atomic structures are performed until forces of are less than 0.003 eV/Å. For surfaces, all atoms in the top two atomic layer along with any adsorbates are optimized. For bulk IrO₂ and RuO₂, cell parameter optimization is also done.

The BEEF-vdW² exchange correlation functional with the vdW-DF2³ nonlocal correlation energy and potential is used here to properly represent adsorbate interactions^{4,5}. Van der Waals effects are important for larger adsorbate molecules formed in CO₂ reduction⁶. When multiple adsorption geometries are possible, different configurations are evaluated to identify the energetically most favorable one; e.g. the CHO* intermediate, which prefers binding simultaneously through the O and C atoms. For a bridge site between an Ir and a Ru atom, the adsorbate O atom can bind to the Ru atom and C atom to the Ir atom or vice versa (figure SI1).

The adsorption geometry can be such that the Ru-Ir bond is perpendicular to the C-O bond of the CHO* adsorbate. The free energy of the reactant and product molecules are calculated by including zero point energy and finite temperature contributions to the free energy within the quantum mechanical harmonic approximation, as described in previous computational studies of CO₂RR on oxide surfaces⁷. Specific parameters for molecular free energy calculations like fugacity and adjustments for systematic DFT errors⁸ used in this work have been listed in the supporting information.

Thermodynamics of electrochemical CO2RR

To estimate the change in free energy under an applied potential for elementary proton transfer steps, the reaction thermodynamic are calculated using the computational hydrogen electrode (CHE) model⁹. CHE provides a simple linear model to evaluate the effect of applied potential on the reaction free energy of an elementary electrochemical reaction step⁹ at a certain applied potential from the reaction free energy, calculated without explicitly including the potential or the electrolyte system. The model links the reaction free energy of each reduction step involving single proton transfer (ΔG_{step}) to the applied potential (U) by a simple linear relation

$$\Delta G_{\text{step}}(U) = \Delta G_{\text{step}}(U = 0) + eU$$

Where e is the elementary charge. If a reaction step involving a proton/electron transfer increase the free energy by $\Delta G_{\text{step}}(U = 0)$ eV, on the reversible hydrogen electrode (RHE) scale, applying $-\Delta G_{\text{step}}/e$ V-RHE potential, will make the free energy change zero, equilibrating the reaction step. The potential at which all elementary step of a reaction mechanism becomes downhill in free energy (exergonic) is defined as the thermodynamic onset potential. Working with the computational hydrogen electrode model and the RHE scale, large-scale analysis of adsorbate and surfaces becomes manageable.

Adsorbate binding free energies can be used to calculate free energy changes without applied potential $\Delta G_{\text{step}}(U = 0)$, with respect to the free energy of the reference molecules (CO_2 , H_2O , and H_2). For example, OCHO^* is a possible reaction intermediate formed after the first proton transfer starting from CO_2 . The electronic energy of the catalyst surface is E_* and that of the surface with OCHO^* is E_{OCHO^*} . The free energy correction term combining the zero point energy, heat capacity and entropy for the OCHO^* adsorbate is $G_{\text{OCHO}^*}^{\text{corr}}$. The binding free energy of OCHO^* is

$$\Delta G_{\text{OCHO}^*} = E_{\text{OCHO}^*} + G_{\text{OCHO}^*}^{\text{corr}} - E_* - G_{\text{CO}_2} - 0.5 \times G_{\text{H}_2}$$

G_{CO_2} , $G_{\text{H}_2\text{O}}$ and G_{H_2} are the free energy of CO_2 , H_2O and H_2 molecules, respectively. The free energy correction term $G_{\text{OCHO}^*}^{\text{corr}}$ is calculated on $\text{RuO}_2(110)$ surface without spectators and assumed constant irrespective of the spectator coverage or surface chemistry. Finite temperature energy corrections for adsorbates are calculated from the vibrational modes of the adsorbates within the quantum mechanical harmonic approximation. Calculated heat capacity (C_p), entropy as well as zero point energy (E_{ZPE}) are incorporated in the correction term for adsorbates:

$$G^{\text{corr}} = E_{\text{ZPE}} + \int C_p dT - TS$$

The free energies of molecules are calculated within the ideal gas approximation. A previously described method^{7,10} has been followed. The specific calculation parameters and energies are provided in the supporting information. Energies of molecular CO_2 , COOH^* intermediate and molecular H_2 are corrected by +0.3 eV, +0.15 eV and +0.1 eV, respectively, to correct for the systematic DFT errors associated with these species⁸.

The change in free energy associated with an elementary reaction step gives the reaction free energy change at 0 V vs RHE. For example, the free energy change for protonation of the H_2CO^* intermediate to H_3CO^* at 0 V vs RHE is

$$\Delta G_{\text{H}_2\text{CO}^* \rightarrow \text{H}_3\text{CO}^*} = \Delta G_{\text{H}_3\text{CO}^*} - \Delta G_{\text{H}_2\text{CO}^*}$$

The free energy change for protonation of H_3CO^* to methanol is related to the binding free energy of H_2CO^* and reactant H_2 and product CH_3OH .

$$\Delta G_{\text{H}_3\text{CO}^* \rightarrow \text{CH}_3\text{OH}} = G_{\text{CH}_3\text{OH}} - \frac{1}{2}G_{\text{H}_2} - \Delta G_{\text{H}_3\text{CO}^*}$$

The binding energy of CO^* spectators has been reported here with respect to the CO molecule rather than CO_2 .

$$\Delta G_{\text{CO}^*} = E_{\text{CO}^*} + G_{\text{CO}^*}^{\text{corr}} - E_* - G_{\text{CO}}$$

Ir/Ru character ratio

The surfaces are assigned a representative numerical value to indicate how much Ir/Ru-character an adsorbate feels while attached to an active site. This serves as a surrogate variable for mapping binding characteristics and catalytic properties to mixed oxide systems with variable composition. To create a reference point for distribution function analysis, a hydrogen atom is added to the bridge site of the bare oxide surface and geometry optimization is done for the H^* and top two atom layers. The partial radial distribution function (RDF) for Ir and Ru atoms are computed up to 12 Å from the H^* adsorbate which is comparable to the thickness of the simulation slab. Periodic boundary condition is used while estimating the RDF functions. The Ir distribution curve is denoted $\text{Ir}_{\text{rdf}}(r)$ and that of Ru atoms as $\text{Ru}_{\text{rdf}}(r)$. Furthermore, a proxy variable describing abundance of Ir and Ru atoms (Ir_{index} and Ru_{index}) close to the adsorption site is defined as

$$\text{Ru}_{\text{index}} = \int_0^{12} (12 - r)\text{Ru}_{\text{rdf}}(r)dr$$

$$\text{Ir}_{\text{index}} = \int_0^{12} (12 - r)\text{Ir}_{\text{rdf}}(r)dr$$

Using these indexes, a single unbiased parameter ranging from 0 to 1 is created

$$\eta = \frac{\text{Ir}_{\text{index}}}{\text{Ir}_{\text{index}} + \text{Ru}_{\text{index}}}$$

The β -value indicates how IrO_2 -like the character of the active site is expected to be. Pure RuO_2 surface has $\beta = 0$ and pure IrO_2 have $\beta = 1$. Surfaces and their β values are listed in **Error! Reference source not found.**

Table S1: Adsorbate/product cases examined at electron transfer step from $0e^-$ to $8e^-$.

1 e^-	2 e^-	3 e^-	4 e^-
OHCO^* , H^* , COOH^*	HCOOH^* , $\text{CO}^* + \text{H}_2\text{O}(\text{l})$, $\text{HCOOH}(\text{aq})$, $\text{H}_2(\text{aq})$	H_2COOH^* , $\text{CHO}^* + \text{H}_2\text{O}(\text{l})$, $\text{COH}^* + \text{H}_2\text{O}(\text{l})$	$\text{H}_3\text{CO}^* + \text{OH}^*$, $\text{H}_2\text{CO} + \text{H}_2\text{O}(\text{l})$, $\text{O}^* + \text{CH}_3\text{OH}(\text{aq})$, $\text{CHOH}^* + \text{H}_2\text{O}(\text{l})$, $\text{C}^* + 2\text{H}_2\text{O}(\text{l})$
5 e^-	6 e^-	7 e^-	8 e^-
$\text{H}_3\text{CO}^* + \text{H}_2\text{O}(\text{l})$, $\text{H}_2\text{COH}^* + \text{H}_2\text{O}(\text{l})$, $\text{OH}^* + \text{CH}_3\text{OH}(\text{aq})$, $\text{CH}^* + 2\text{H}_2\text{O}(\text{l})$	$\text{O}^* + \text{CH}_4(\text{aq}) + \text{H}_2\text{O}(\text{l})$, $\text{CH}_3\text{OH}^* + \text{H}_2\text{O}(\text{l})$, $\text{CH}_3\text{OH}(\text{aq}) + \text{H}_2\text{O}(\text{l})$, $\text{CH}_2^* + 2\text{H}_2\text{O}(\text{l})$	$\text{OH}^* + \text{CH}_4(\text{aq}) + \text{H}_2\text{O}(\text{l})$, $\text{CH}_3^* + 2\text{H}_2\text{O}(\text{l})$	$\text{CH}_4(\text{aq}) + 2\text{H}_2\text{O}(\text{l})$

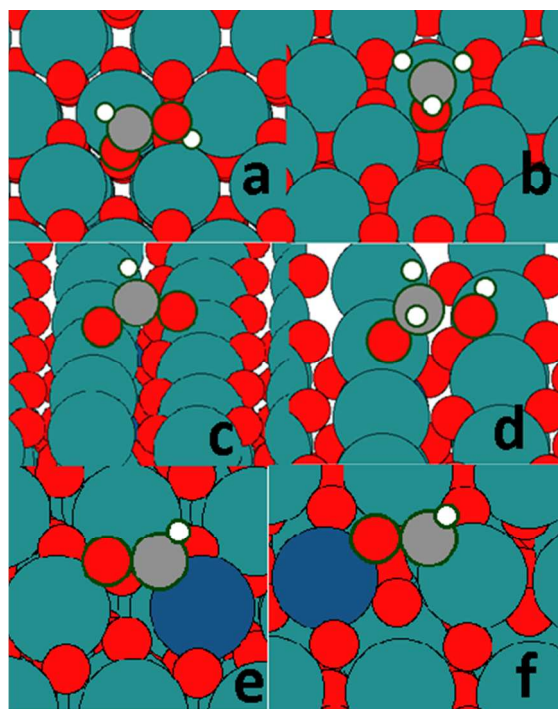
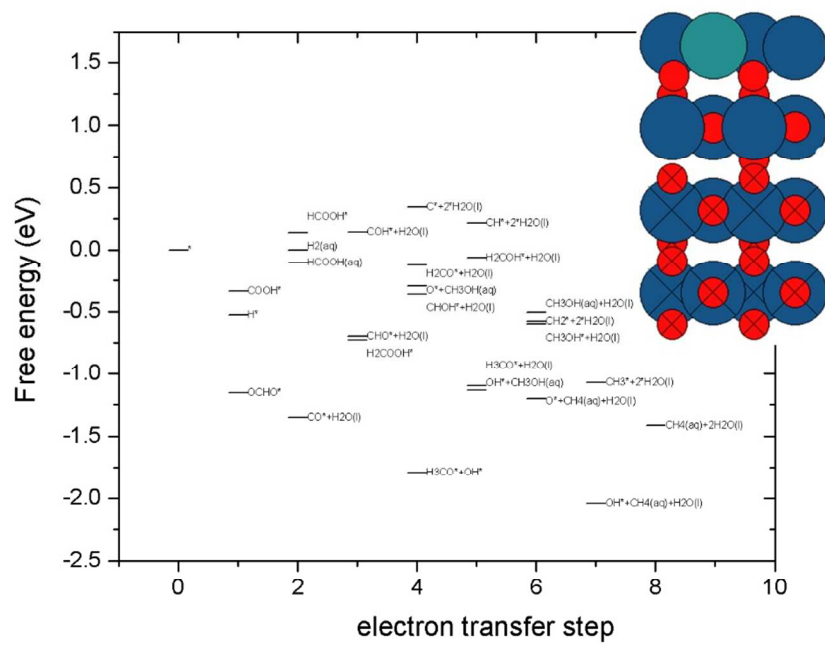
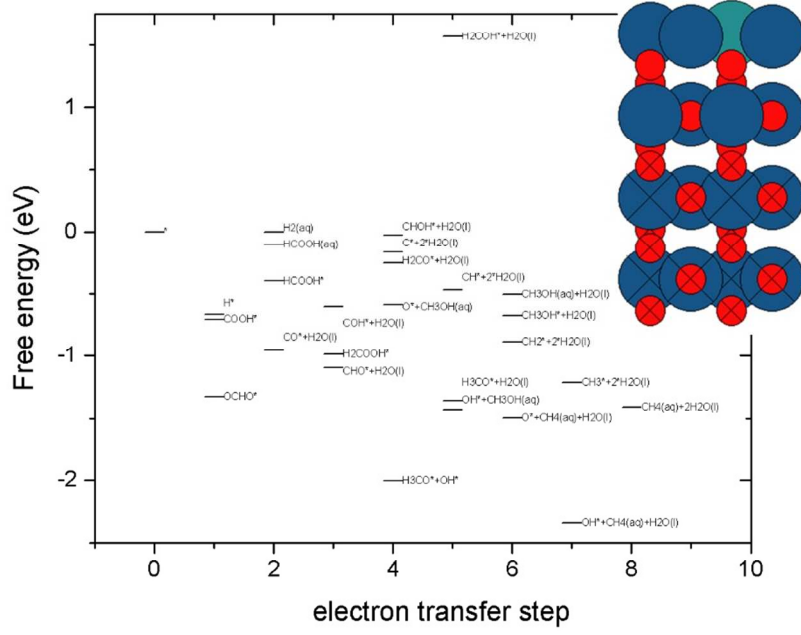
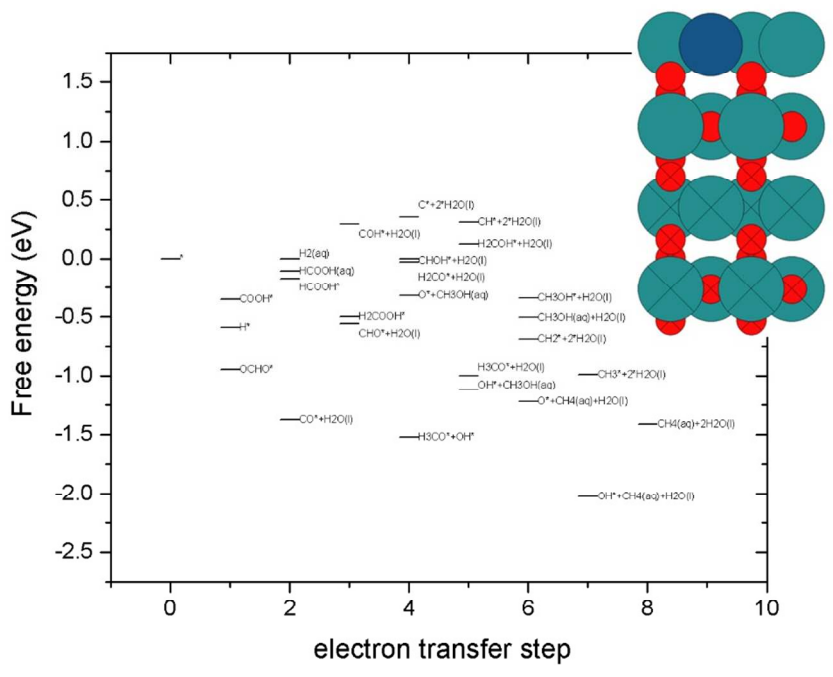
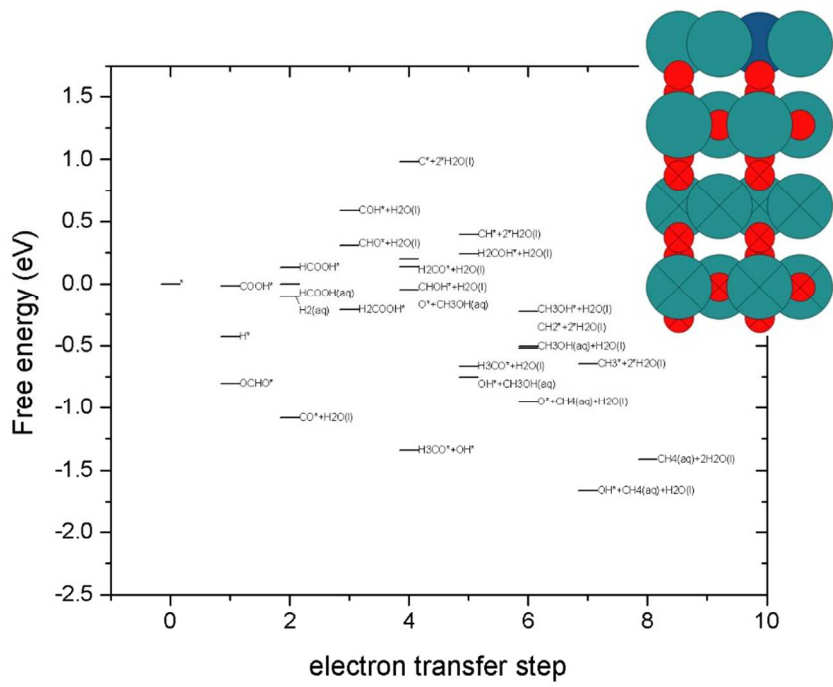


Figure S1: Adsorption geometry of adsorbates (a) HCOOH^* (b) H_3CO^* (c) OCHO^* (d) H_2COOH^* adsorbates on RuO_2 (110) surface and (e)-(f) CHO^* adsorbate in two different configuration on RuO_2 (110) surface with Ir atom substitution close to bridge site





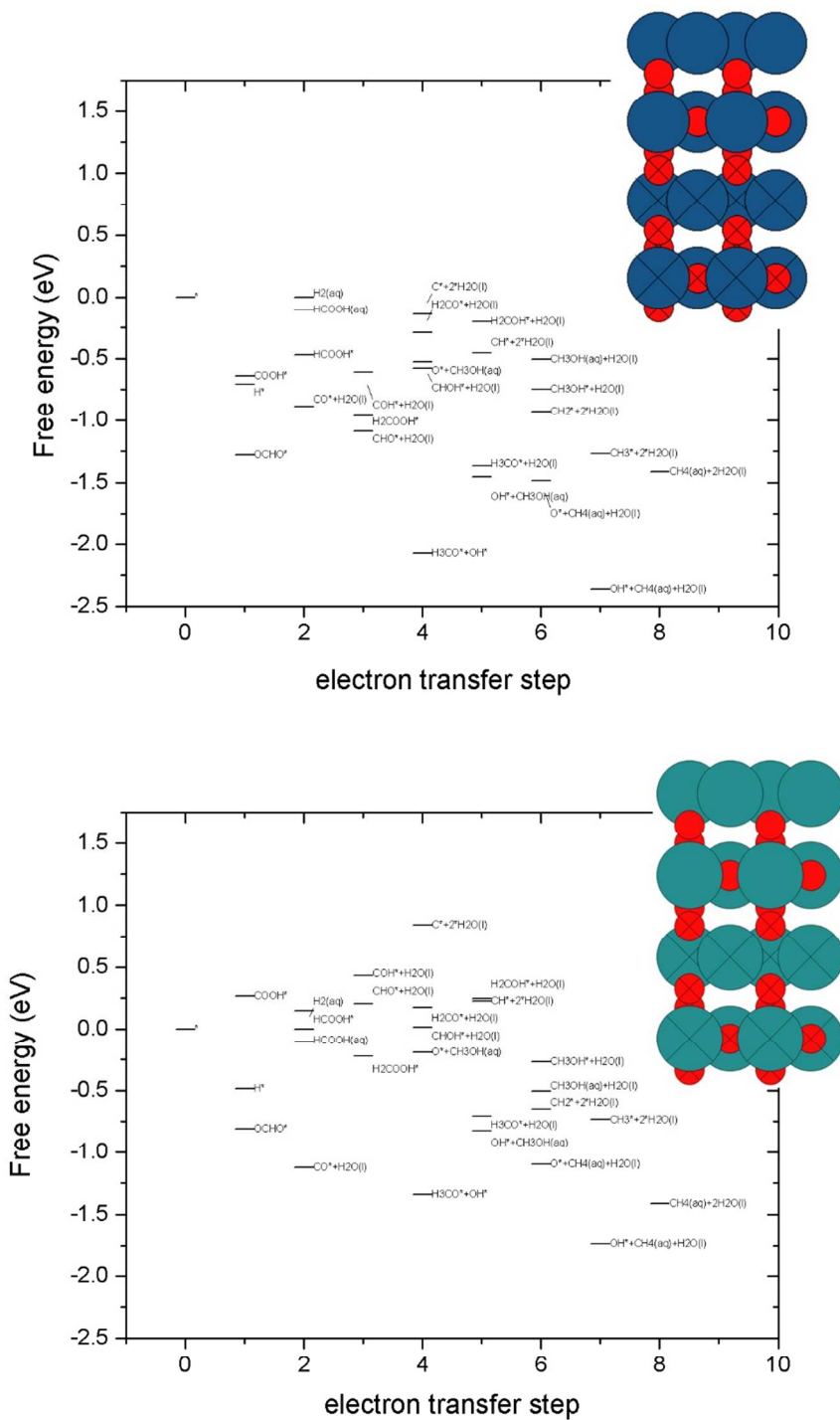
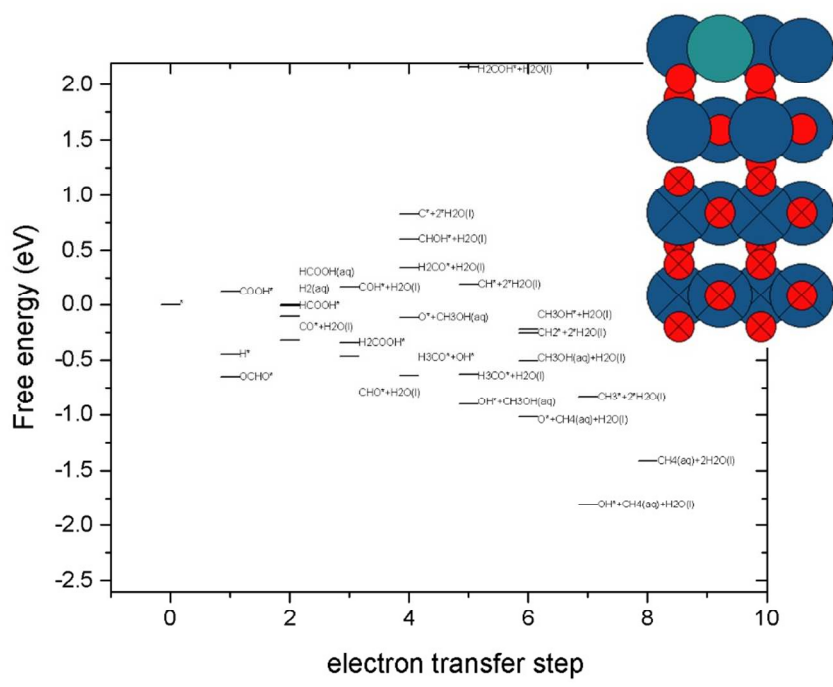
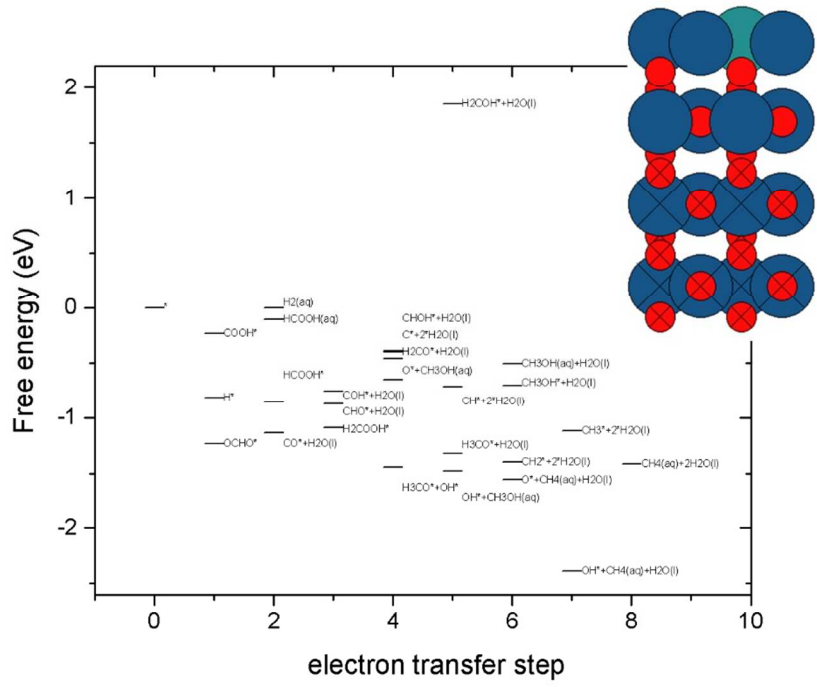
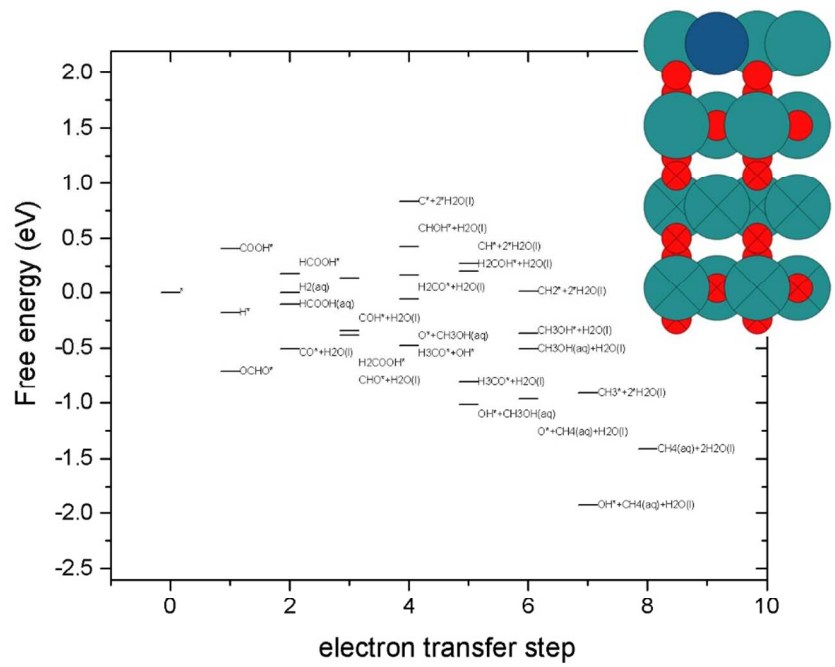
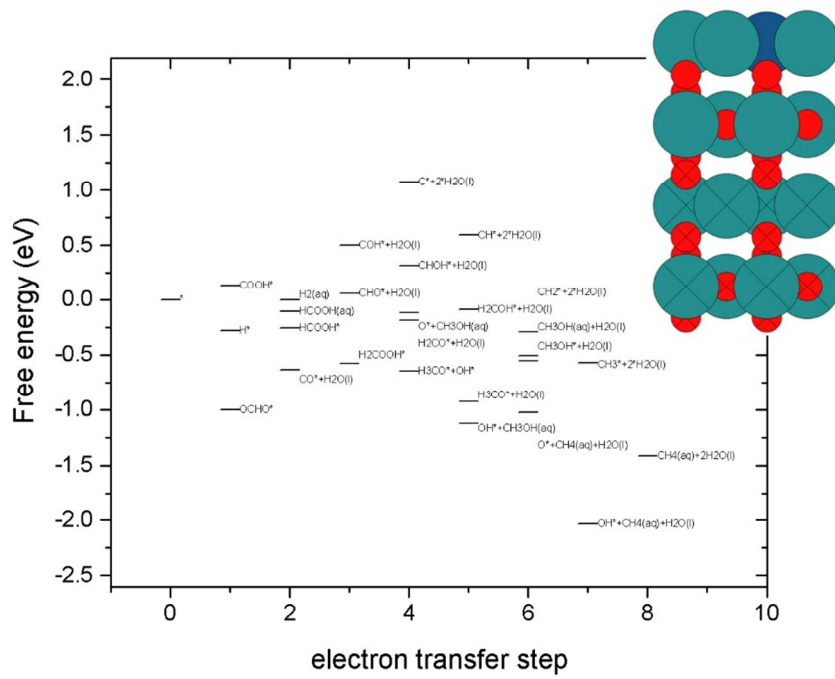
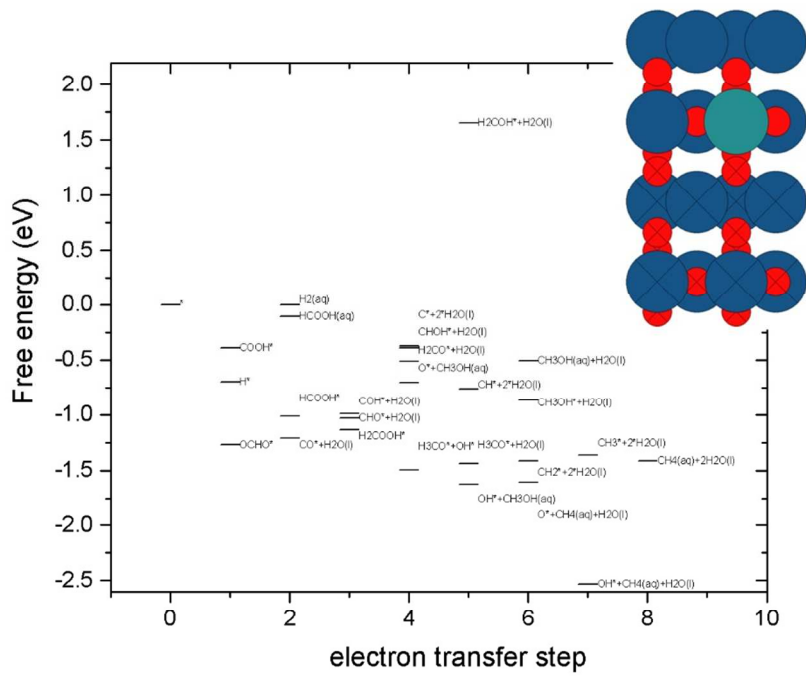
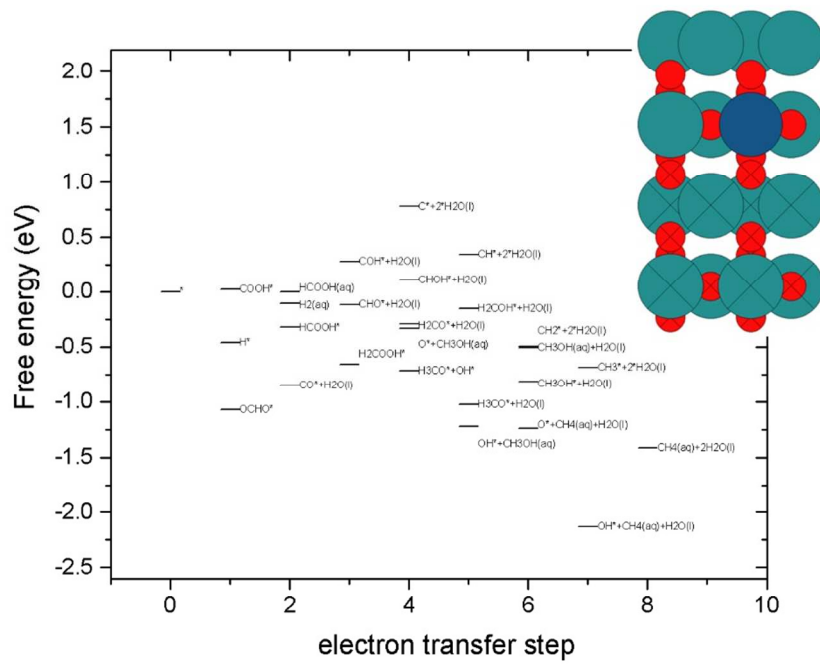
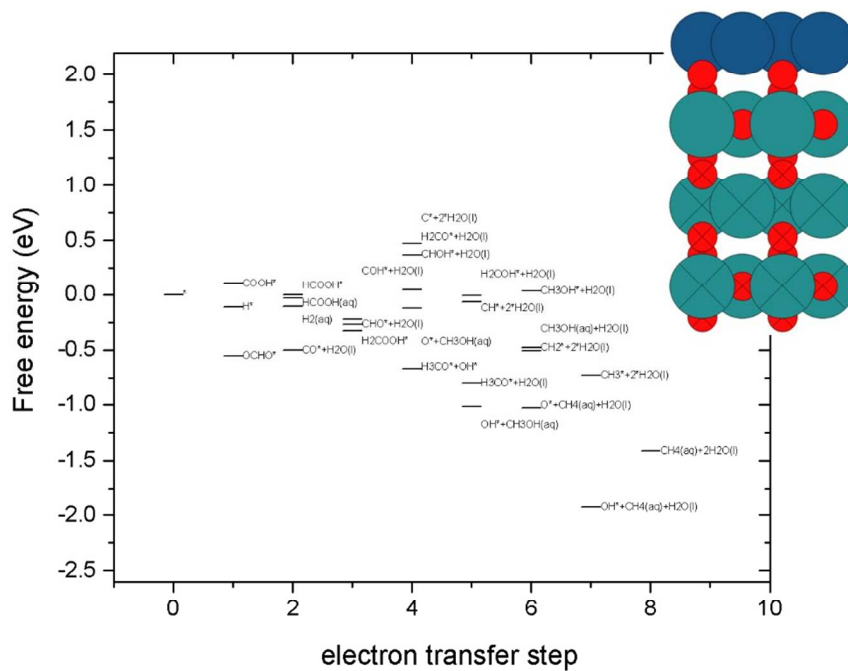
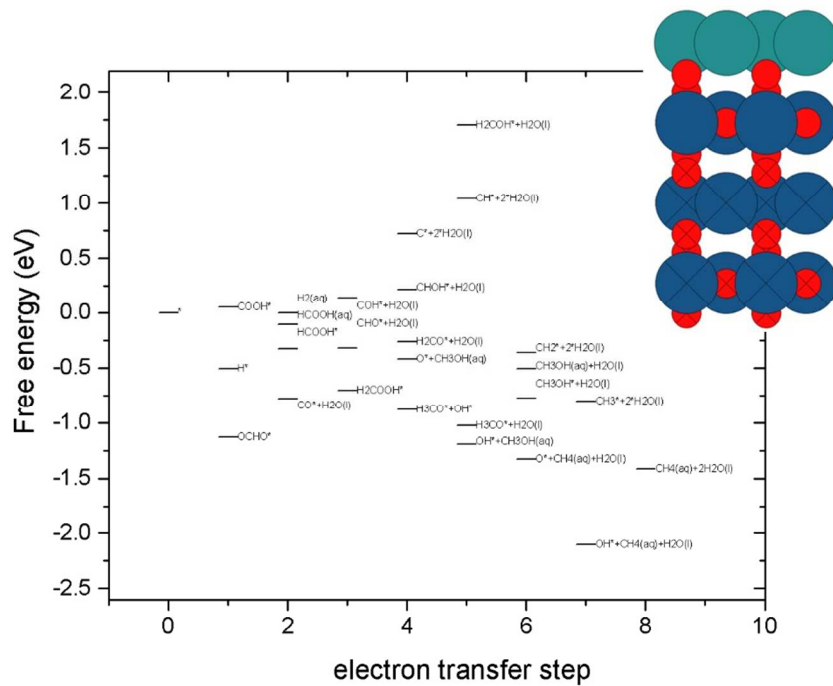


Figure S2: free energy of reaction intermediates and products with reference to CO₂, H₂ and H₂O at 0 V-RHE on all 10 surfaces models with no CO* coverage









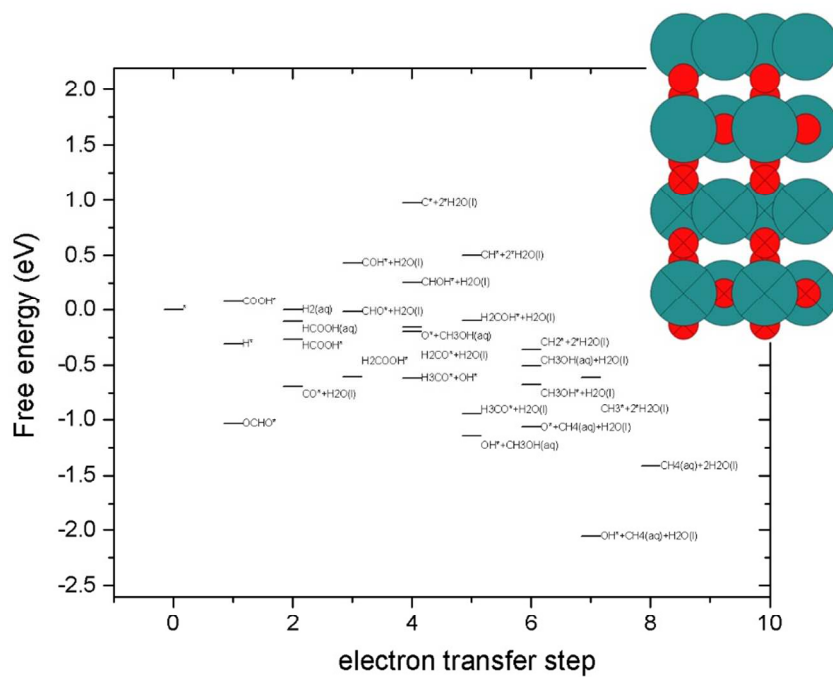
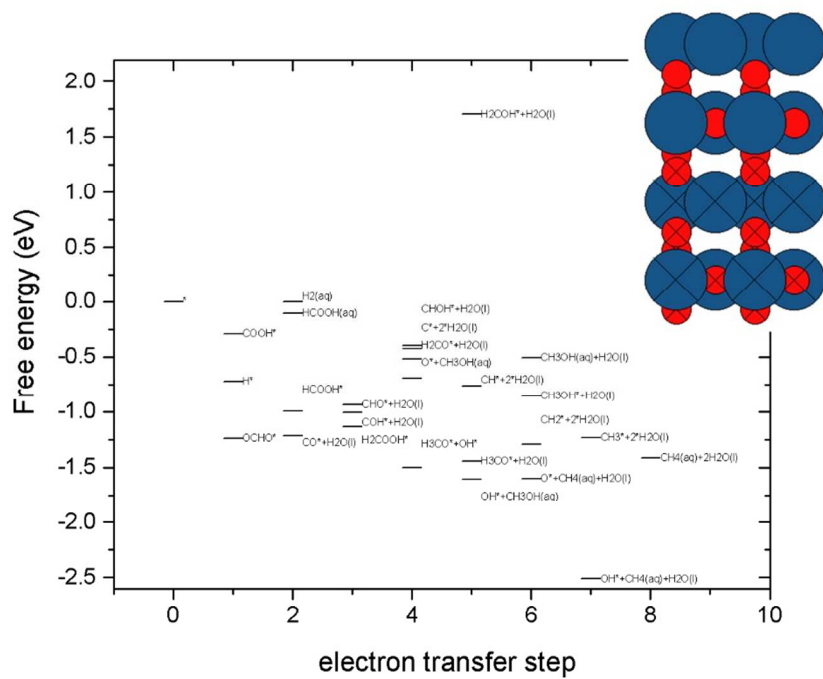
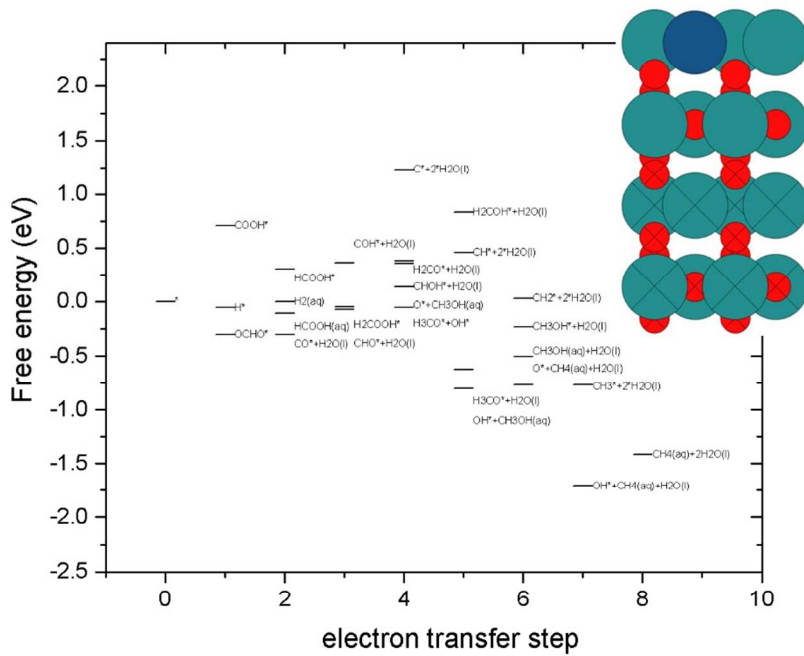
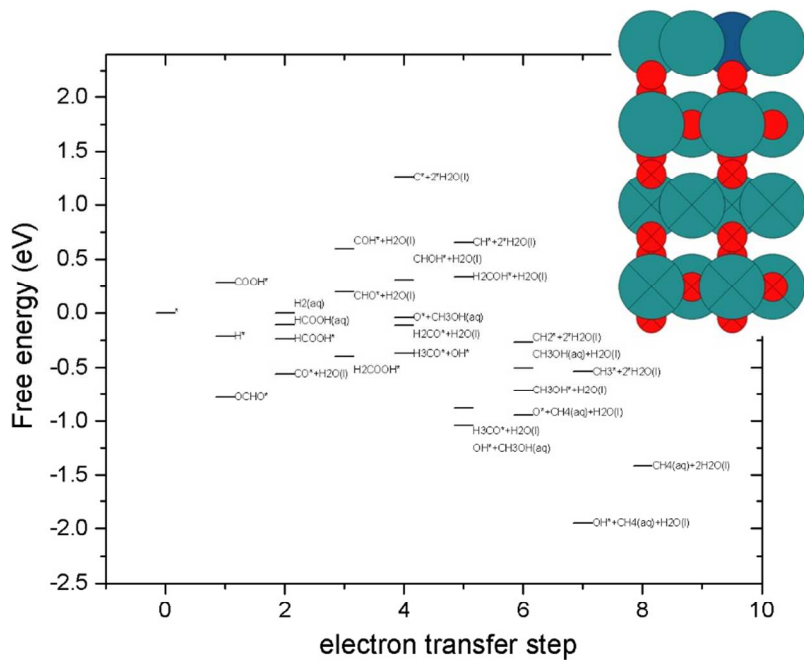
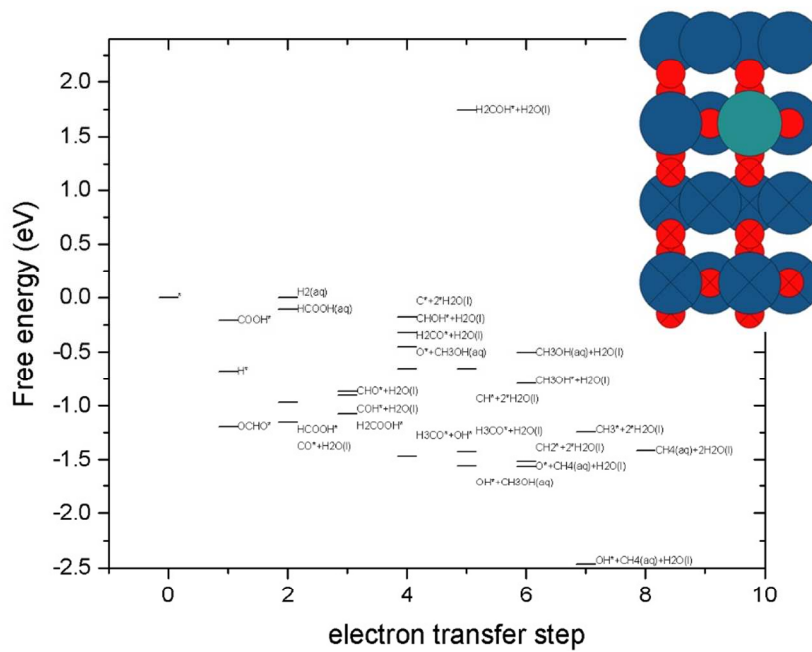
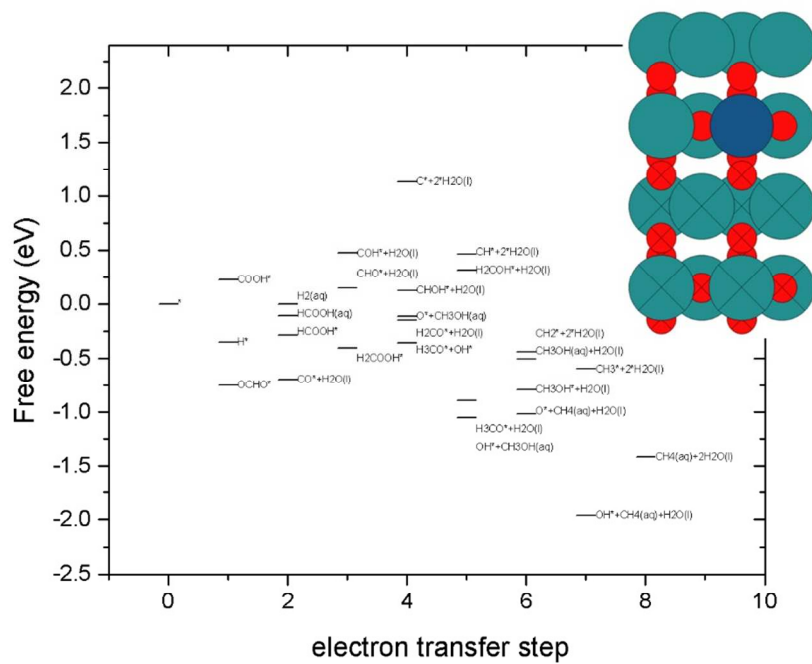


Figure S3: free energy of reaction intermediates and products with reference to CO_2 , H_2 and H_2O at 0 V-RHE on all 10 surfaces models with 25% CO^* coverage





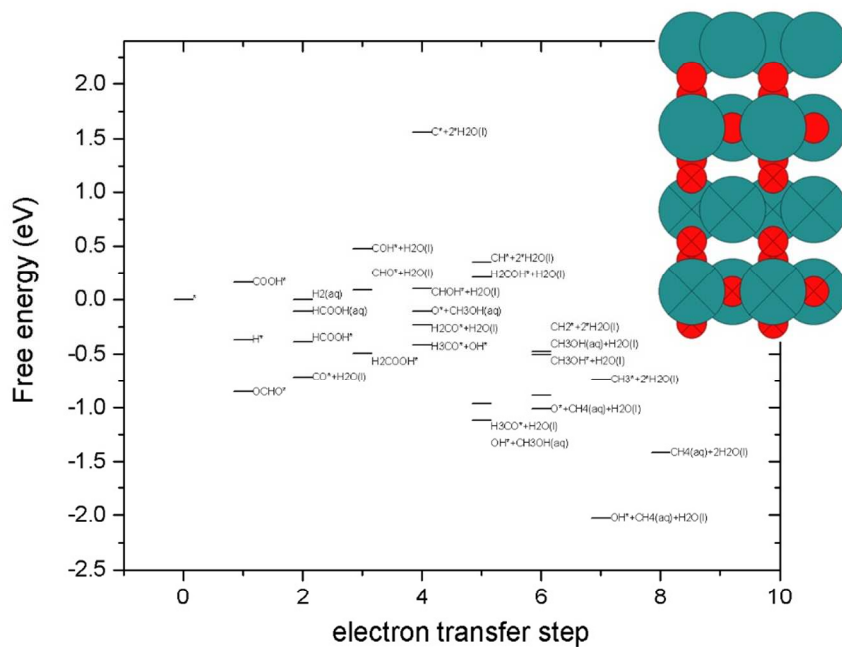
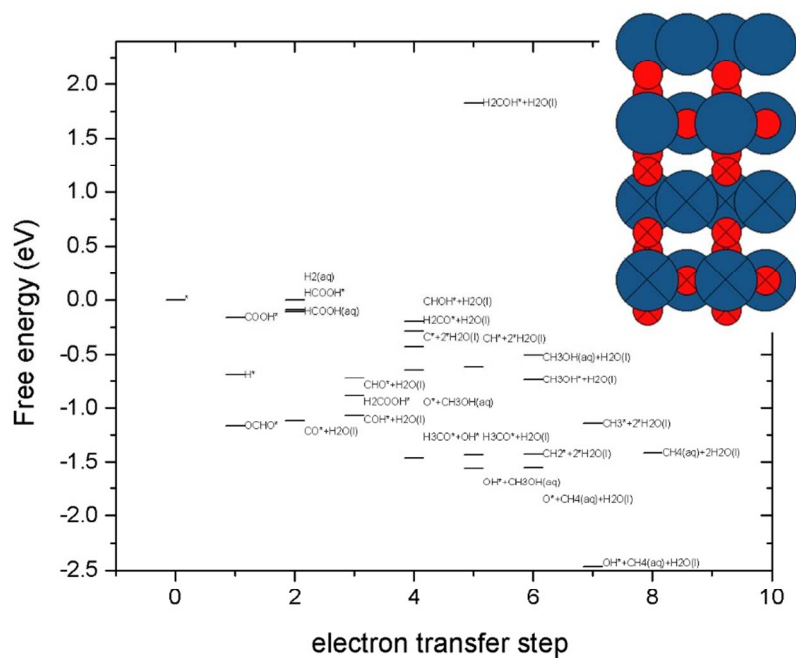
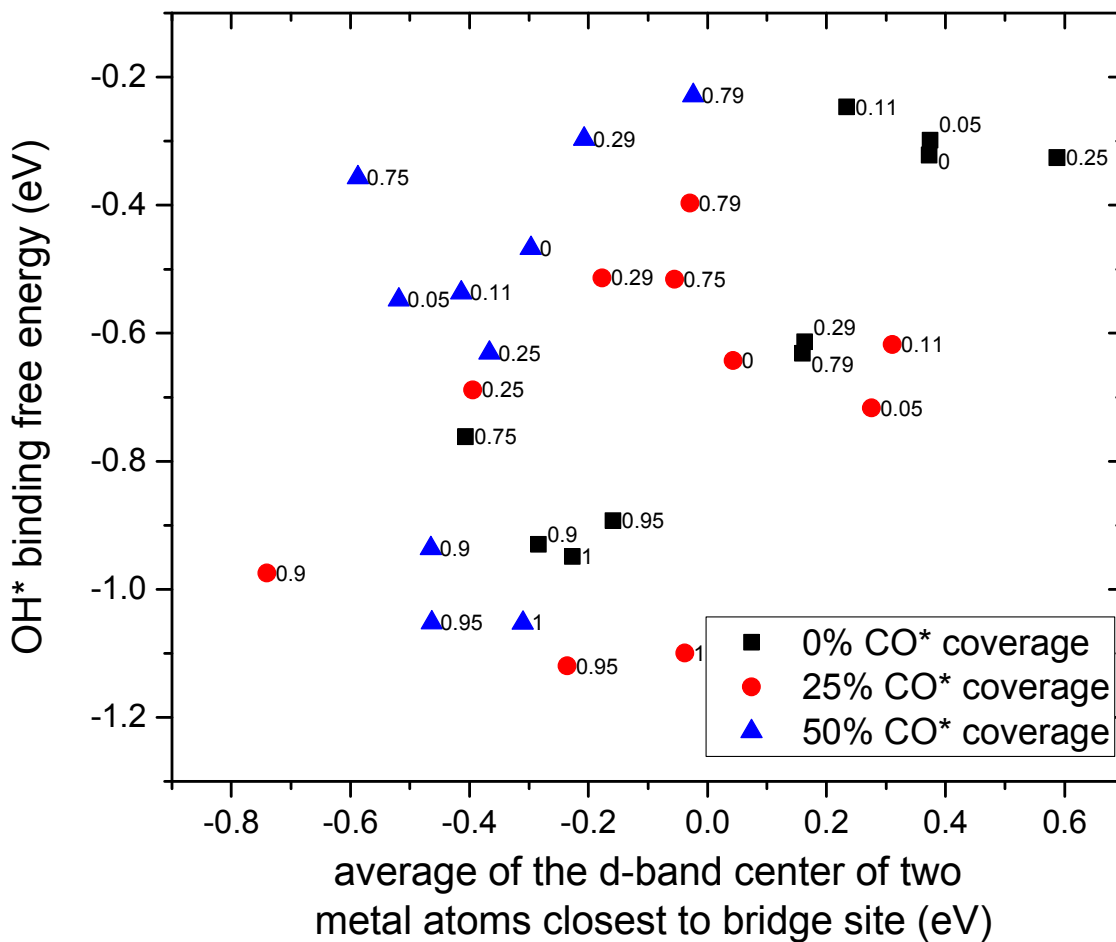


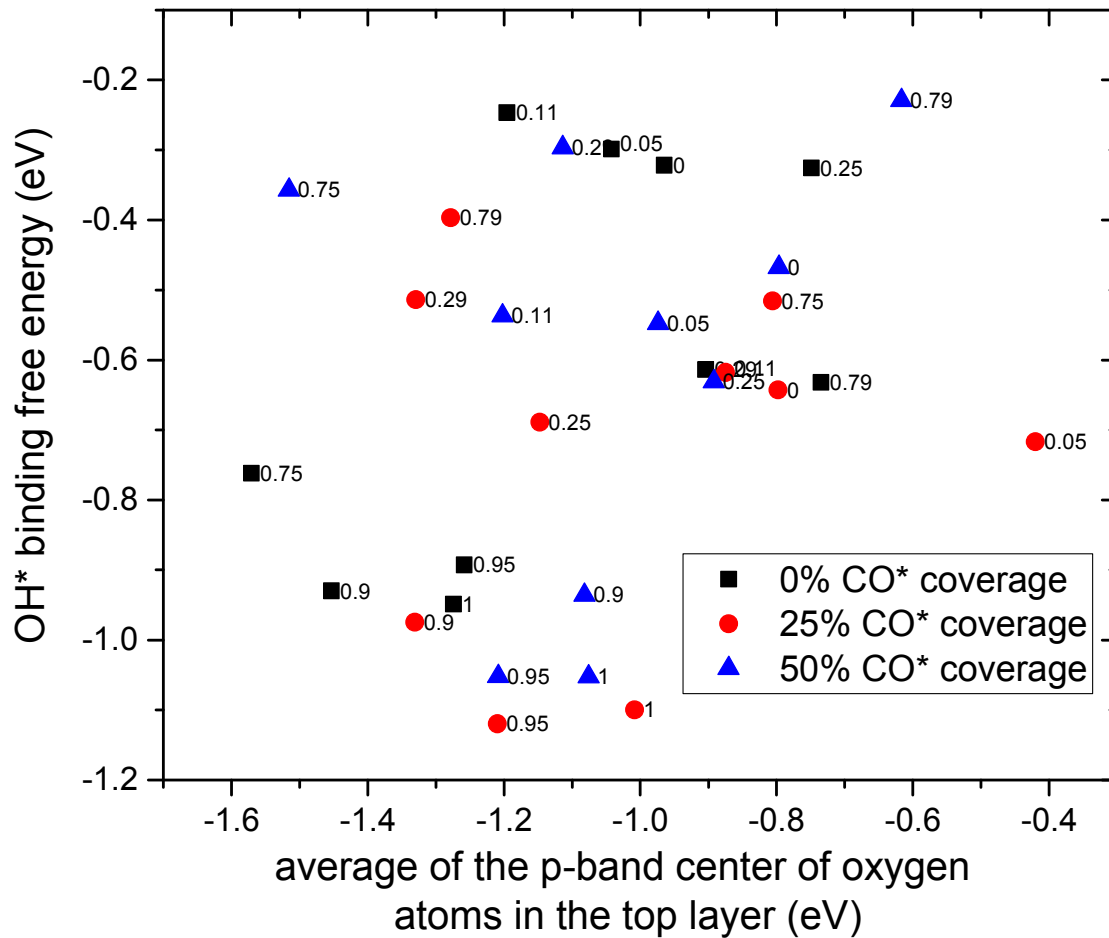
Figure S4: free energy of reaction intermediates and products with reference to CO_2 , H_2 and H_2O at 0 V-RHE on all 10 surfaces models with 50% CO^* coverage

Table S2: Binding free energy difference of COOH* and OCHO* intermediates formed from CO₂ activation. Lightest shade means highest value and darkest is the lowest value (OCHO* more stable).

β	0.00	0.05	0.11	0.25	0.29	0.75	0.79	0.90	0.95	1.00
CO* spectator coverage	OCHO* and COOH* binding free energy difference (eV)									
0%	-1.08	-0.64	-0.78	-1.00	-0.60	-0.67	-0.82	-0.62	-0.66	-0.64
25%	-1.11	-1.10	-1.14	-1.18	-1.12	-0.66	-0.78	-1.00	-0.88	-0.94
50%	-1.01	-0.98	-1.06	-1.01	-1.01	-0.51	-0.83	-1.01	-0.99	-1.00

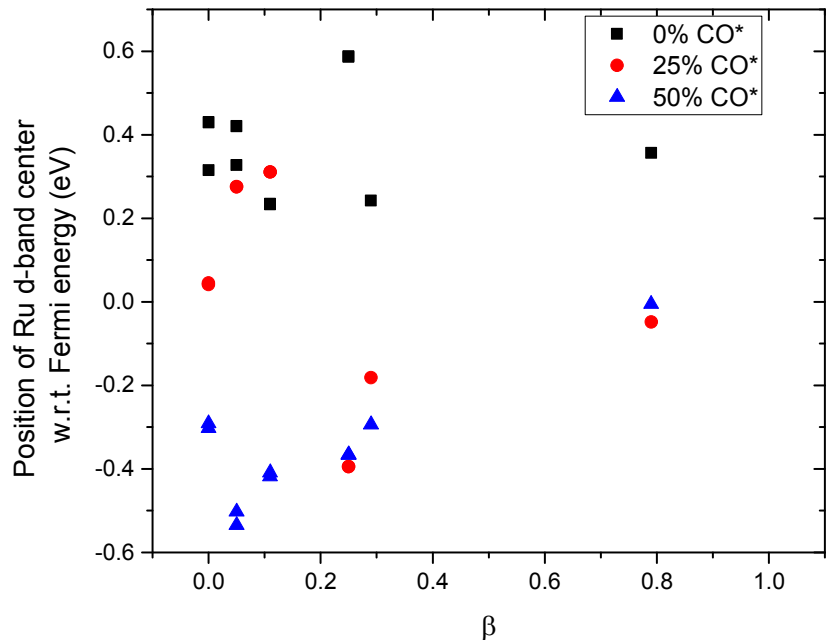


(a)

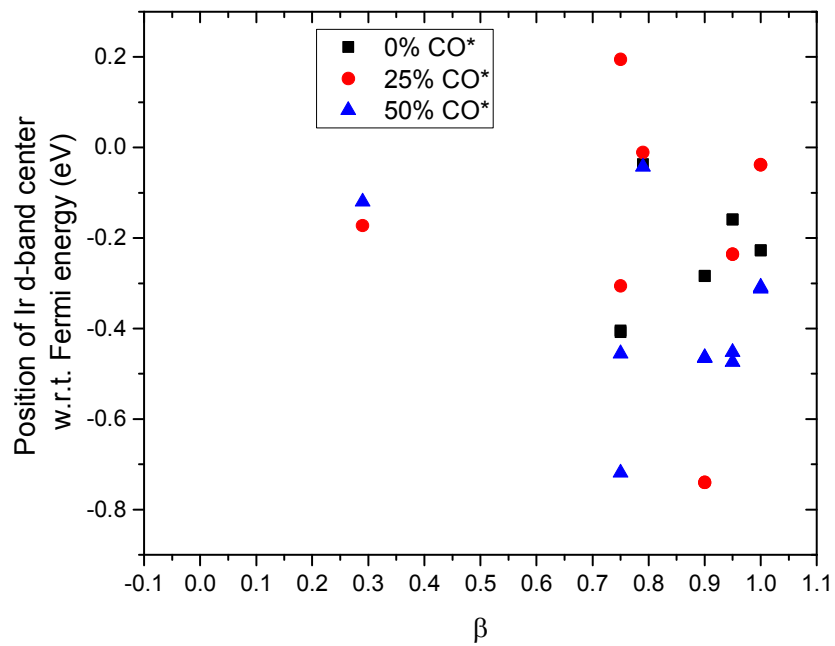


(b)

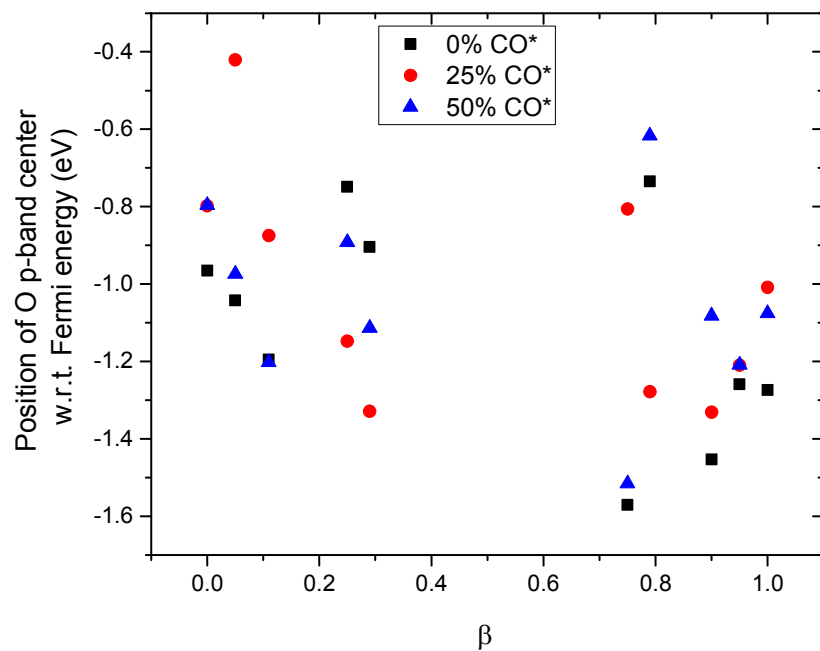
Figure S5: correlation of OH* binding free energy with (a) average d-band position of the two metal atoms closest to the bridge site (b) average p-band position of oxygen atoms in the top layer of the catalyst surfaces. Labels indicate the β value of the surface for which the data point.



(a)

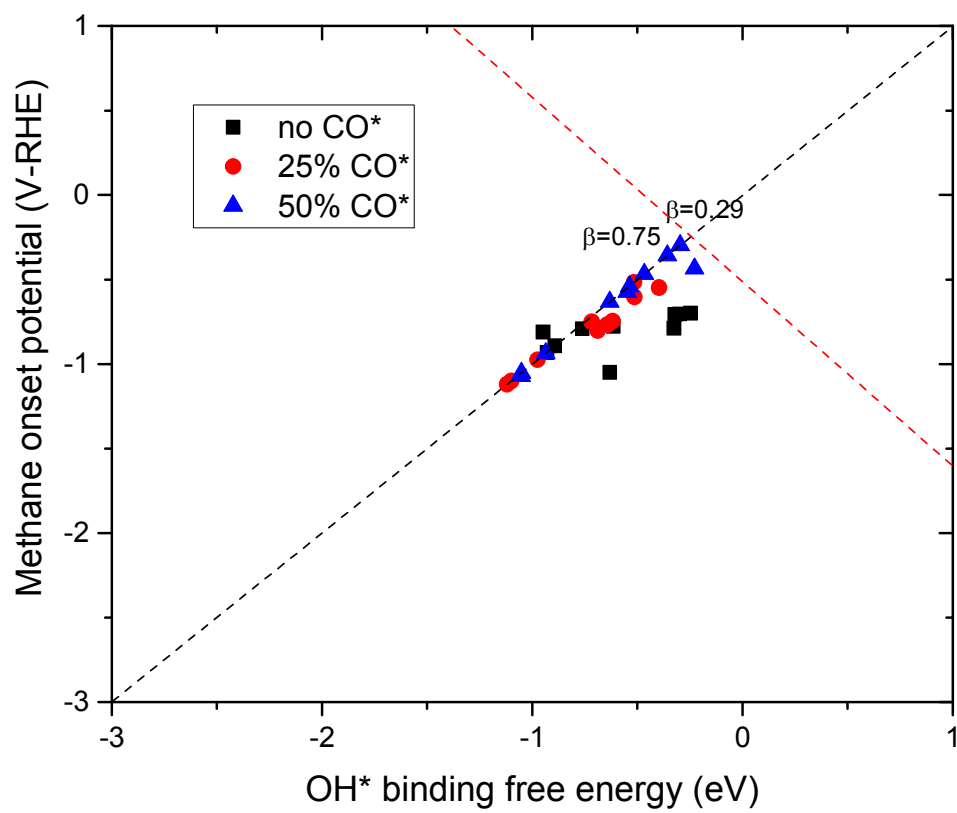


(b)

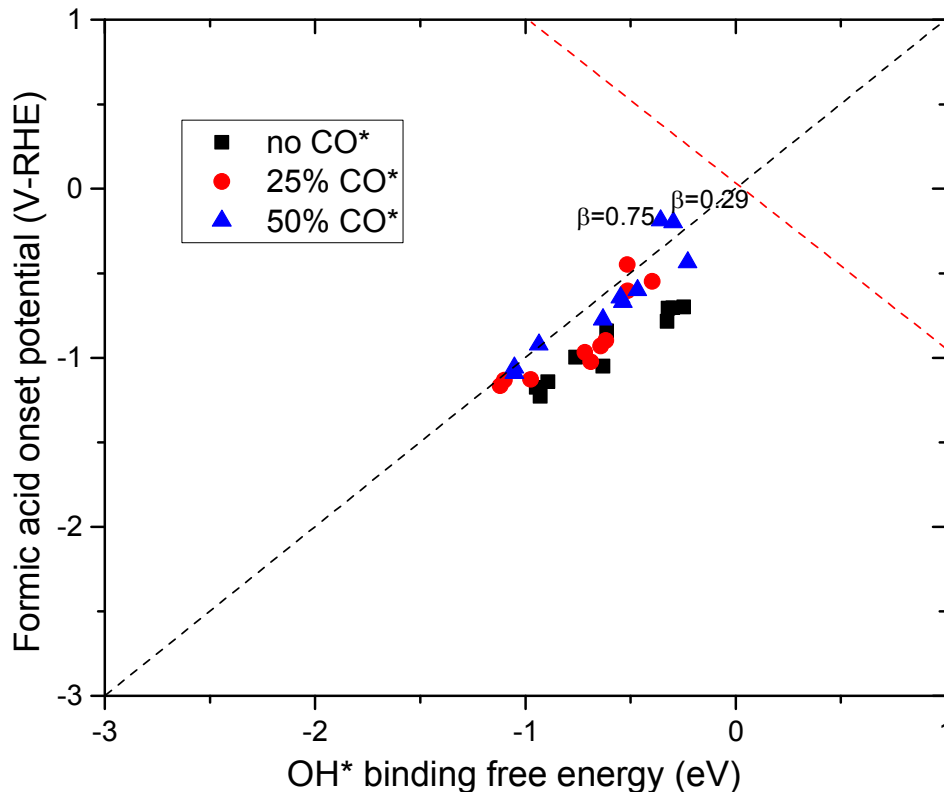


(c)

Figure S6: Modification in the band center for (a) Ru-d electrons (b) Ir d-electrons (c) O-p electrons, due to ligand effects and CO* coverage



(a)



(b)

Figure S7: Effects of ligand interaction and adsorbate-adsorbate interaction from spectating CO* moves partially CO* covered mixed Ir-Ru oxide surfaces closer to the top of the volcano for oxide catalysts (a) methane (b) formic acid evolution. Activity volcanos for different products obtained from our previous work⁷.

References:

- (1) Kresse, G. *Phys. Rev. B* **1999**, *59*, 1758–1775.
- (2) Wellendorff, J.; Lundgaard, K. T.; Møgelhøj, A.; Petzold, V.; Landis, D. D.; Nørskov, J. K.; Bligaard, T.; Jacobsen, K. W. *Phys. Rev. B* **2012**, *85*, 235149.
- (3) Lee, K.; Murray, É. D.; Kong, L.; Lundqvist, B. I.; Langreth, D. C. *Phys. Rev. B - Condens. Matter Mater. Phys.* **2010**, *82*, 3–6.
- (4) Liu, W.; Carrasco, J.; Santra, B.; Michaelides, A.; Scheffler, M.; Tkatchenko, A. *Phys. Rev. B - Condens. Matter Mater. Phys.* **2012**, *86*, 1–6.
- (5) Ramalho, J. P. P.; Gomes, J. R. B.; Illas, F. *RSC Adv.* **2013**, *3*, 13085.
- (6) Studt, F.; Abild-Pedersen, F.; Varley, J. B.; Nørskov, J. K. *Catal. Letters* **2013**, *143*, 71–73.
- (7) Bhowmik, A.; Vegge, T.; Hansen, H. A. *ChemSusChem* **2016**, *9*, 3230–3243.

- (8) Christensen, R.; Hansen, H. A.; Vegge, T. *Catal. Sci. Technol.* **2015**, *5*, 4946–4949.
- (9) Nørskov, J. K.; Rossmeisl, J.; Logadottir, A.; Lindqvist, L.; Kitchin, J. R.; Bligaard, T.; Jónsson, H. *J. Phys. Chem. B* **2004**, *108*, 17886–17892.
- (10) Hjorth Larsen, A.; Jørgen Mortensen, J.; Blomqvist, J.; Castelli, I. E.; Christensen, R.; Dułak, M.; Friis, J.; Groves, M. N.; Hammer, B.; Hargus, C.; Hermes, E. D.; Jennings, P. C.; Bjerre Jensen, P.; Kermode, J.; Kitchin, J. R.; Leonhard Kolsbjerg, E.; Kubal, J.; Kaasbjerg, K.; Lysgaard, S.; Bergmann Maronsson, J.; Maxson, T.; Olsen, T.; Pastewka, L.; Peterson, A.; Rostgaard, C.; Schiøtz, J.; Schütt, O.; Strange, M.; Thygesen, K. S.; Vegge, T.; Vilhelmsen, L.; Walter, M.; Zeng, Z.; Jacobsen, K. W. *J. Phys. Condens. Matter* **2017**, *29*, 273002.